International Journal of Earth Sciences
https://doi.org/10.1007/s00531-018-1606-x

ORIGINAL PAPER

Regional deformation of late Quaternary fluvial sediments in the Apennines foreland basin (Emilia, Italy)

Marco Stefani[1,2] · **Luca Minarelli**[2] · **Alessandro Fontana**[3] · **Irka Hajdas**[4]

Received: 2 July 2017 / Accepted: 18 March 2018

Abstract
Our research is aimed at estimating the vertical deformation affecting late Quaternary units accumulated into the foreland basin of the Northern Apennines chain. Beneath the study alluvial plain, compressive fault-fold structures are seismically active. We reconstructed the stratigraphic architecture and the depositional evolution of the alluvial deposits, which accumulated in the first 40 m of subsurface, through the last 45,000 years, from before the Last Glacial Maximum to the present. A 58 km-long stratigraphic profile was correlated from the foothill belt near Bologna to the vicinity of the Po River. The analysis of the profile documents subsidence movements through the last 12,000 years, exceeding − 18 m in syncline areas, with subsidence rates of at least 1.5 m/ka. Anticlines areas experienced a much lower subsidence than the syncline ones.

Keywords Subsidence · Foreland basin · Fluvial depositional system · Stratigraphy · Pleistocene · Holocene · Po Plain · Italy

Introduction

In tectonically active sedimentary basins, syndepositional deformation plays a key role in the shaping of the depositional architecture. Active foreland basins generally register both fast subsidence and large sediment input, generating a comprehensive stratigraphic record. This is the case of the Po Plain area, corresponding to the shared foreland basin of the Southern Alps and the Northern Apennines (Fig. 1).

During the Quaternary, compressive deformation and subsidence have been particularly active in the southern portion of the basin (Emilia-Romagna Region), in areas corresponding to the buried frontal structures of the Apennines (Boccaletti et al. 2004; Martelli et al. 2017). In the year 2012, the region was stricken by several earthquakes ("Geological framework"). While the recent seismic activity and the coseismic topographic movements are well documented by seismography and radar interferometry data ("Geological framework"), the deformation of the buried Quaternary units is more difficult to assess. The study of these units can, however, play an important role in providing a longer temporal perspective for the interpretation of the region deformation and seismicity. Our work is, therefore, aimed at providing the first quantitative estimation of the vertical displacements recorded by late Pleistocene and Holocene units, buried in the south-eastern portion of the Po Plain. The research investigates a transept stretching between the Northern Apennines foot hills and the southern portion of the Holocene Po River channels belt, crossing an area strongly affected by the 2012 earthquakes (Fig. 1). The study is based on the reconstruction of the depositional architecture and of the post-depositional deformation of the sedimentary bodies, buried in the first 40 m of subsurface. The reconstruction derives from the correlation of about 5500 subsurface logs, within a chronological framework integrating more than 60

✉ Marco Stefani
stm@unife.it

Luca Minarelli
minarelli@geotema.it

Alessandro Fontana
alessandro.fontana@unipd.it

Irka Hajdas
hajdas@phys.ethz.ch

[1] Dipartimento di Architettura, Università degli Studi di Ferrara, Via Quartieri 8, 44121 Ferrara, Italy

[2] Geotema, Via Piangipane 141/5, 44121 Ferrara, Italy

[3] Dipartimento di Geoscienze, Università degli Studi di Padova, Via Grandenigo 6, 35131 Padova, Italy

[4] Laboratory of Ion Beam Physics, ETH, HPK H25, Otto-Stern-Weg 5, 8093 Zurich, Switzerland

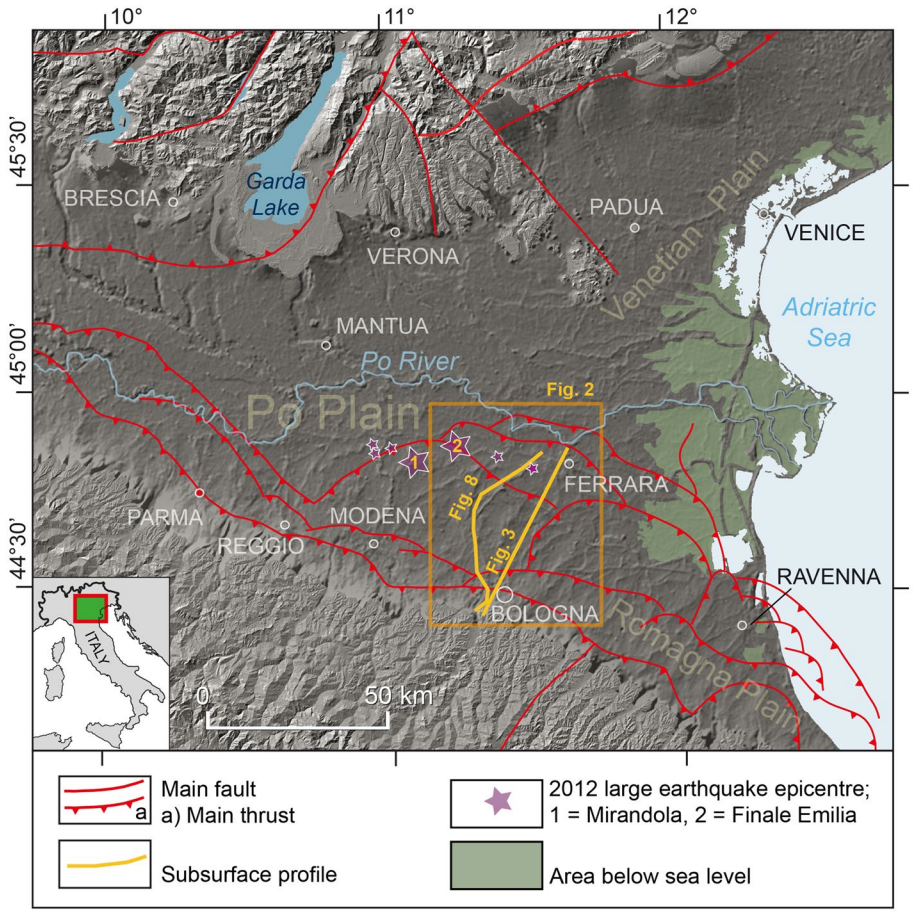

Fig. 1 Regional framework of study area, part of the tectonic active Apennines foreland basin of northern Italy. The map depicts the topographic relief of the region, the main tectonic structures of the basin, and the epicentres of the 2012 largest earthquakes. The location of the map of Fig. 2, of the structural section of Fig. 3, and of the regional stratigraphic profile B–B′ of Fig. 8 area also depicted

^{14}C measurements. We are going to discuss the sedimentological and geomorphological evolution of the depositional environments over the last 45,000 years. The research documents large lateral gradient of subsidence, showing a strong relationship with the underlying active tectonic structures.

Geological framework

The research deals with the south-eastern portion of the Po Plain, between the towns of Bologna, Modena, and Ferrara (Fig. 1). The densely populated area corresponds to the alluvial plain of the Reno and Po rivers. The topographic surface of the study plain gently dips northward, from the Apennines foothill to the drainage axis of the Po River, varying in elevation from 70 to 6 m a.s.l., over a distance of about 55 km (Figs. 1, 2). The region corresponds to the south-eastern part of the foreland basin, developed between the collisional chains of the Alps and Apennines (Fig. 1). The compressional structures of the external portion of the Northern Apennines are active beneath the study alluvial plain. The fault-fold system (Fig. 3), generated during late Tertiary and Quaternary times, involves the sedimentary Mesozoic and Cenozoic cover, which is detached from the Variscan basement (Pieri and Groppi 1981; Toscani et al. 2009; Boccaletti et al. 2011).

The Plio-Pleistocene successions accumulated during the deformation of these structures and record great lateral variations in both sedimentary facies and stratigraphic thickness (Ghielmi et al. 2010; Martelli et al. 2017). The vertical movements associated with the active deformation of the fault-fold structures are superimposed to a fast regional subsidence, related with the northward propagation of the Apennine thrust belt (Carminati et al. 2005). Within the general subsiding trend of the region, the syncline belts have recorded much larger subsidence rates than the anticline ones (Boccaletti et al. 2011; Ghielmi et al. 2010; Martelli et al. 2017). The Quaternary units record the development of several discordance and non-deposition surfaces, which were induced by both tectonic deformation and glacio-eustatic fluctuations (Amorosi et al. 1999). The discordance surfaces support the subdivision of the sedimentary successions into unconformity bounded units, as synthems and subsynthems. The latter correspond to transgressive–regressive depositional cycles, influenced by the glacio-eustatic fluctuations (Regione Emilia-Romagna et al. 1998). The sediments belonging to the last complete cycle are framed into the AES7 Villa

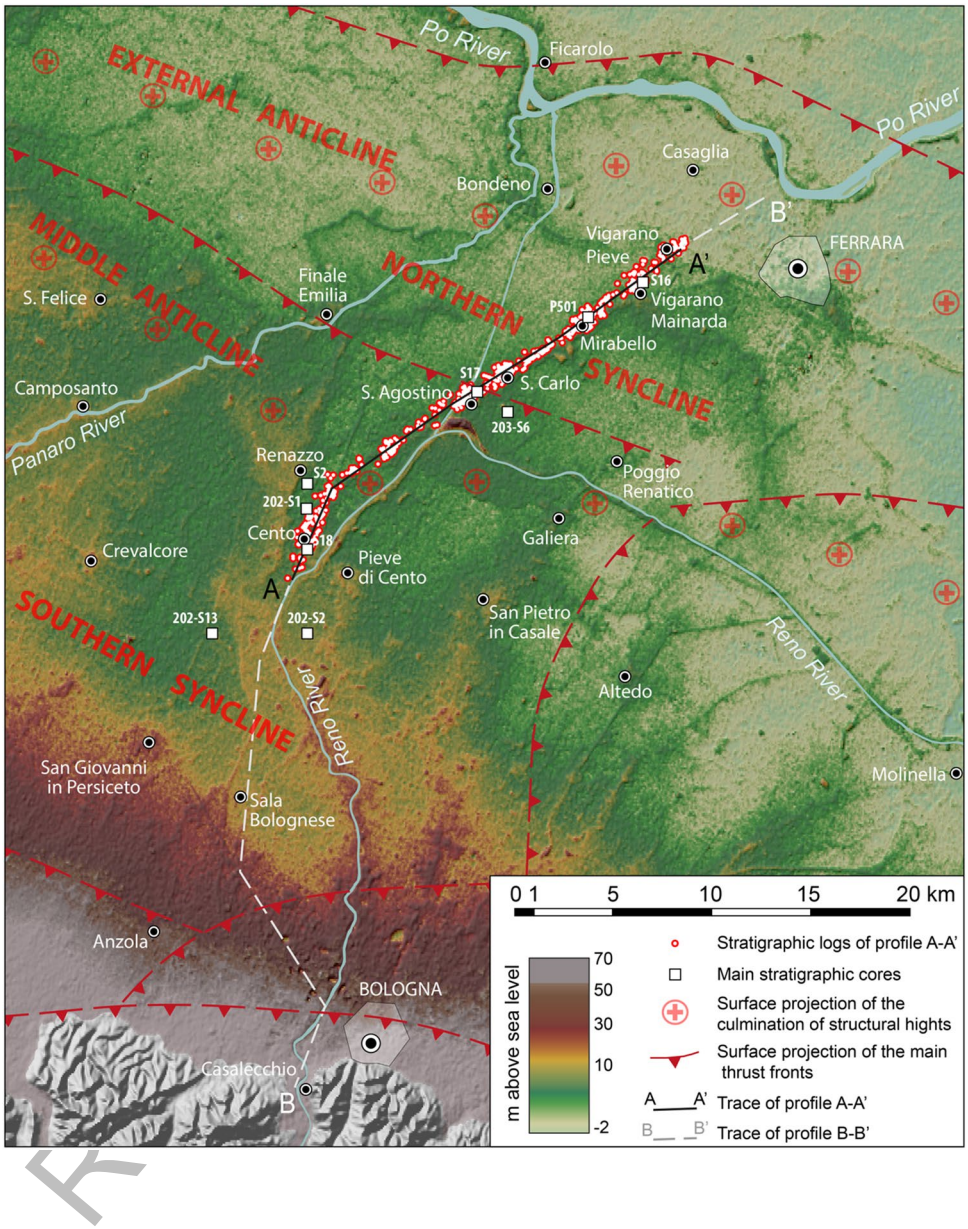

Fig. 2 Elevation model of the study region. The alluvial plain shows elongated fluvial ridges, interspaced with interfluvial depressions. The location of the main buried overthrusts and anticlines is depicted in a simplified way. The map represents the position of the stratigraphic cores correlated in Fig. 5, of the high-resolution stratigraphic profile A–A′ of Fig. 7, and of the regional profile B–B′ of Fig. 8. The profile A–A′ is stretched along the Reno River palaeochannel ridge and is based on the correlation of 961 subsurface logs, depicted by the superposed dots. Squared symbols indicate the position of the stratigraphic cores correlated in Fig. 5

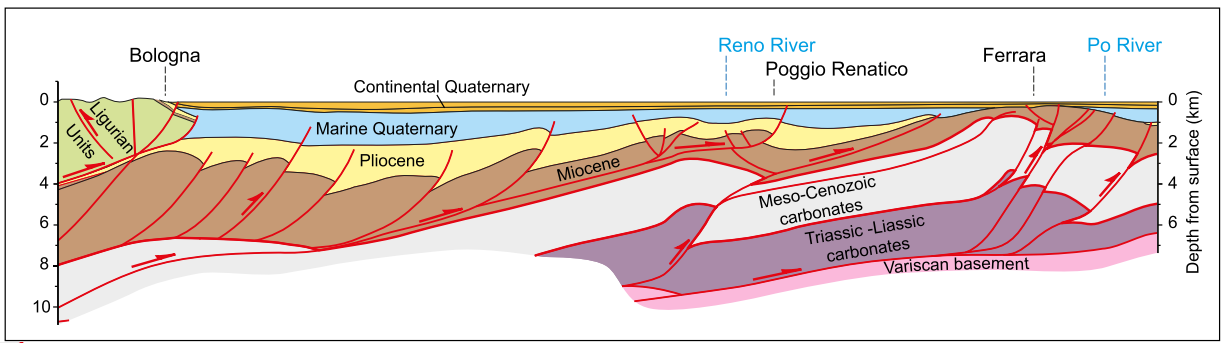

Fig. 3 Structural profile crossing the research region, modified from Boccaletti et al. (2004). The Meso-Cenozoic cover is detached from the metamorphic basement and involved into active compressive deformation. Two complex anticline structures are associated with ramp overthrusts, interspaced by two large synclines. For location, see Fig. 1

Verrucchio Subsynthem. The AES7 unit includes the sediments deposited during the Last Glacial Maximum (LGM, *sensu* Clark et al. 2009) and the late glacial period. The post-glacial sediments have been ascribed to the Ravenna Subsynthem (AES8), the base of which roughly correlates to the beginning of the Holocene. The entirety of the outcropping sediments is ascribed to the younger portion of the subsynthem, which, in the research region, is dominated by the channel bodies of the Po, Reno, and other minor rivers outflowing the Apennines (Fig. 4).

In the region, historic sources witness the occurrence of earthquakes since Roman times. Major events are documented (Guidoboni 1987; Guidoboni et al. 2007) near Argenta (1624, 1909 AD), Bologna (1365, 1504–1505, 1666, 1725, 1779, 1929), Ferrara (1346, 1411, 1509, 1561, 1570–1574, 1796), Finale Emilia (1574, 1639, 1908), and Modena (1117, 1249, 1474, 1501, 1660, 1850). Ancient episodes of coseismic liquefaction of sands are documented (Caputo et al. 2012, 2016).

Modern seismological data document a frequent seismic activity, induced by the buried frontal structures of the Apennines and characterized by shallow epicentres, generally at depth of about 10 km or less (Basili et al. 2008; Tertuliani et al. 2009; DISS Working Group 2015). In May 2012, several earthquakes affected the south-eastern portion of the Po Plain (QUEST 2012; Michetti et al. 2012; Pizzi and Scisciani 2012; Saraò and Peruzza 2012; Tertulliani et al. 2012). The strongest shock (M_L 5.9) happened the 20th of May, at a hypocentre depth of about 6.3 km. The same day, another event (M_L 5.1) was generated, at the south-eastern outskirt of Ferrara (Vigarano Mainarda, Fig. 1). The second largest earthquake (M_L 5.8) took place at a western site (Mirandola). The earthquakes were associated with the central anticline belt (Figs. 1, 2, 3), culminating in the Mirandola area

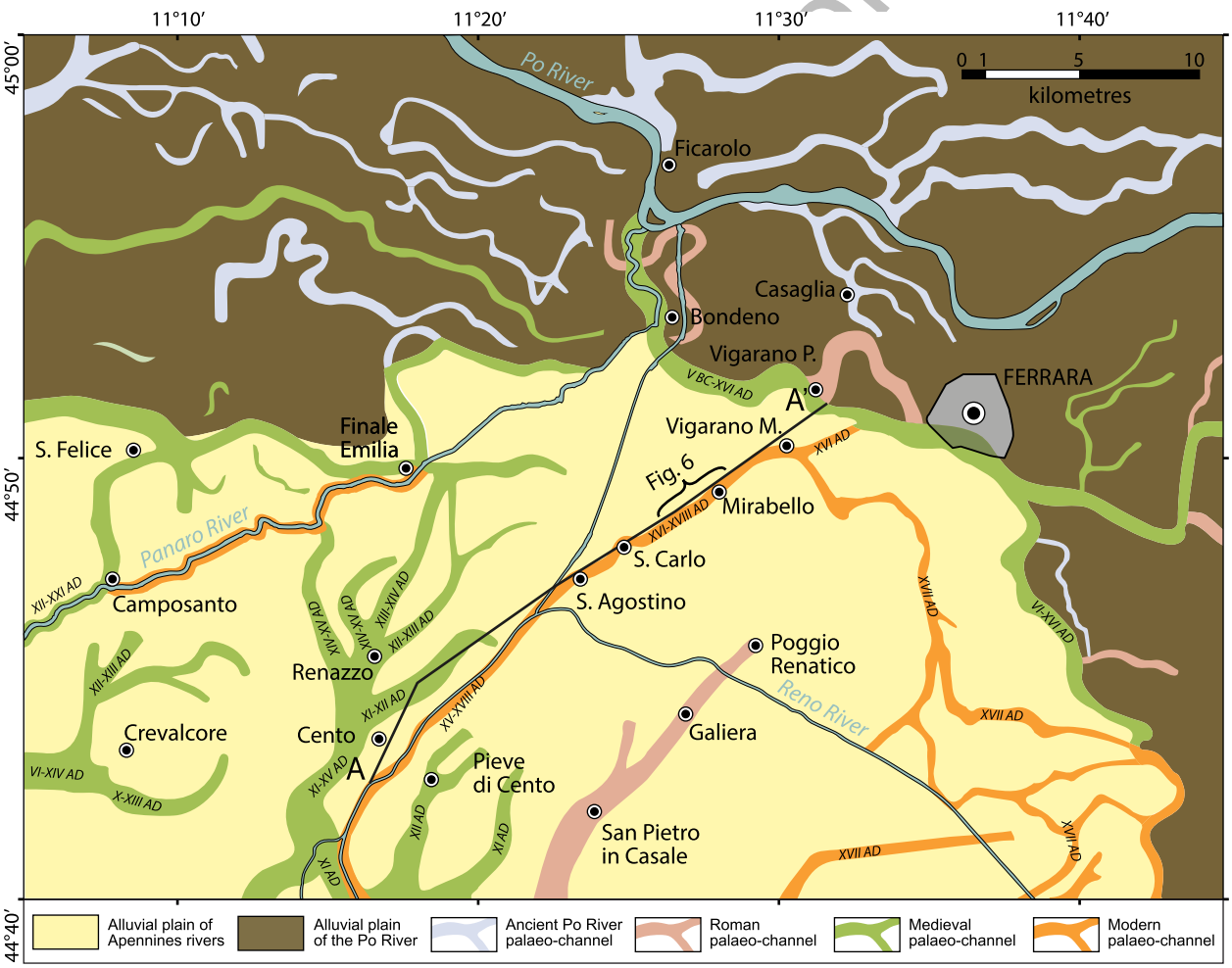

Fig. 4 Main fluvial channel sand bodies outcropping in the central-northern part of the study area. The southern portion of the depicted region is formed by Apennine-derived sediments and the northern area is dominated by the Po River deposits. Map partially based on the map of Castiglioni et al. (1997). Dating of the dipositional centuries of the fluvial channels is given by Roman numbers. The location of the stratigraphic correlation example of Fig. 6 and of the profile A–A′ of Fig. 7 is depicted

(Tarabusi and Caputo 2016). Compressive focal mechanisms were recorded for these earthquakes, with some local strike slip component (Pondrelli et al. 2012; Scognamiglio et al. 2012). The earthquakes generated widespread damage, associated with coseismic liquefaction of fluvial sands (Alessio et al. 2013; Servizio Geologico 2012; Galli et al. 2012). Satellite radar interferometry data document coseismic vertical uplift of up to 25 cm, associated with coseismic subsidence of adjacent areas (Bignami et al. 2012; Caputo et al. 2014; Pezzo et al. 2013).

Data sources and research methods

Subsurface data sources

The research is based on the collection of about 5500 subsurface logs, consisting of stratigraphic logs, cone penetration tests (CPT), piezocone penetration tests (CPTU), geotechnical cores, and water well logs, organized within a GIS database. The pre-existing data have been calibrated through correlation with new continuous stratigraphic cores and seismic piezocone penetration tests (SCPTU), carried out by the Emilia-Romagna Region administration (Regione Emilia-Romagna 2012), the Bologna University (Amorosi et al. 2016a), and our research team (this contribution). Cone penetration testing has demonstrated itself as a powerful tool for stratigraphy interpretation of unlithified sediments (De Mio and Giacheti 2007), as also demonstrated by research on the study region (Amorosi and Marchi 1999; Stefani and Vincenzi 2005). In the cores, the sediments were described according to a standardized procedure (Sanesi 1977; FAO-ISRIC 2006), with attention to palaeosol horizons, which provide good markers for regional correlation (Amorosi et al. 2014, 2016a). Information on outcropping surface and subsurface units derived also from the previous geological maps (CARG project: Amorosi and Severi 2009; Cibin and Segadelli 2009; Gasperi and Pizziolo 2009; Martelli et al. 2009a, b; Molinari and Pizziolo 2009) and by our new mapping of the area between Cento and the Po River (Fig. 4; Stefani and Minarelli 2016). The geomorphology of the area was investigated through airborne laser altimetry (LIDAR), provided by the Regione Emilia Romagna. Published geochronology data were generated by the CARG Project (previous references) and by other authors (Sala and Gallini 2002; Regione Emilia-Romagna 2012; Amorosi et al. 2016a; Bruno et al. 2015, 2016). We dated five samples corresponding to key horizons for correlation (Table 1), using the accelerator mass spectrometry method (AMS), at the ETH Ion Beam Laboratory in Zürich. We recalibrated all available ages in a uniform way, using the OxCal software version 4.2.3 (Bronk Ramsey 2009), with the IntCal-13 atmospheric calibration curves (Reimer et al. 2013). Age estimations are hereafter presented with a precision of 2σ.

Construction of the stratigraphic panel and regional profiles

Subsurface data were mutually correlated to generate the stratigraphic profile A–A′ (Figs. 6, 7), which is 40 m deep and 26 km long. The profile strikes in an NE–SW direction, fairly perpendicularly to the strike of the main tectonic structures. The profile crosses the area strongly affected by the 20th of May 2012 earthquakes, along the Ferrara-Modena road, largely through urbanized areas, maximizing the spatial density of data (Fig. 2). The stratigraphic interpretation is based on 961 subsoil logs, selected within a buffer belt extending for 500 m on both sides of the profile trace. The chronological interpretation of the profile stratigraphy is supported by 20 ^{14}C measurements. A portion of the profile A–A′ is reported in detail in Fig. 6. To frame the interpretation of the profile within a larger regional context, the section was extended both southward and northward with a lower accuracy level, attaining a total length of 58 km (profile B–B′, incorporating a simplified version of the A–A′ one, Figs. 1, 8). Our own stratigraphic correlation of the southern portion of the profile B–B′ was compared with a recently published interpretation of the area (Bruno et al. 2016). The B–B′ profile stretches from the base of the Apennines,

Table 1 Mass spectrometry isotopic ^{14}C dating performed on core samples

Conventional ^{14}C age	Error	Calibrated age 2σ 95.2% prob. (year cal. BP)	Longitude WGS84	Latitude WGS84	Surface elevation (m m.s.l.)	Depth from surface (m)	Corrected elevation (m m.s.l.)	References
4731	30	5584–5327	44°50′35.15"N	11°29′36.49"E	10.00	14.64	−4.64	This paper
3705	29	4149–3972	44°47′39.45"N	11°23′13.94"E	16.00	15.28	0.72	This paper
26,348	153	30,967–30,302	44°47′39.45"N	11°23′13.94"E	16.00	26.62	−10.62	This paper
10,459	40	12,549–12,132	44°43′19.25"N	11°17′0.36"E	17.00	18.4	−1.40	This paper
25,122	117	29,500–28,840	44°43′19.25"N	11°17′0.36"E	17.00	27.95	−10.95	This paper

For stratigraphic location, see Fig. 5. The stratigraphic position of samples is indicated by the letters C written in white in Fig. 5. The geographic position of cores is illustrated in Fig. 1

near Bologna, to the north-western outskirt of Ferrara. The southern portion of the B–B′ profile forms variable angle with the subsurface structural direction, at places significantly reducing the apparent dip. The southern portion of the profile B–B′ shows a large variability of data density. The information is scantier in the countryside between Cento and Sala Bolognese, but is plentiful in the urban sprawl area of Bologna (Fig. 8). The southern portion of the profile B–B′ directly incorporates 13 ^{14}C datings. Further chronological evidence was provided by correlation with 24 more ^{14}C measurements from adjacent areas.

Stratigraphic units and chronological framework

The study sediments accumulated through latest Pleistocene and Holocene times, into fluvial depositional environments, under largely variable climatic and eustatic conditions. These environmental fluctuations induced region-wide discontinuity surfaces and large variations in the sedimentological features, supporting the subdivision of the interval into four informal units (Figs. 5, 7, 8). (1) A single unit frames any sediment below the Glacial deposits, (2) the following unit accumulated during the last glacial maximum and late glacial phases, (3) the lower Holocene syn-transgressive unit is followed by the (4) upper Holocene one.

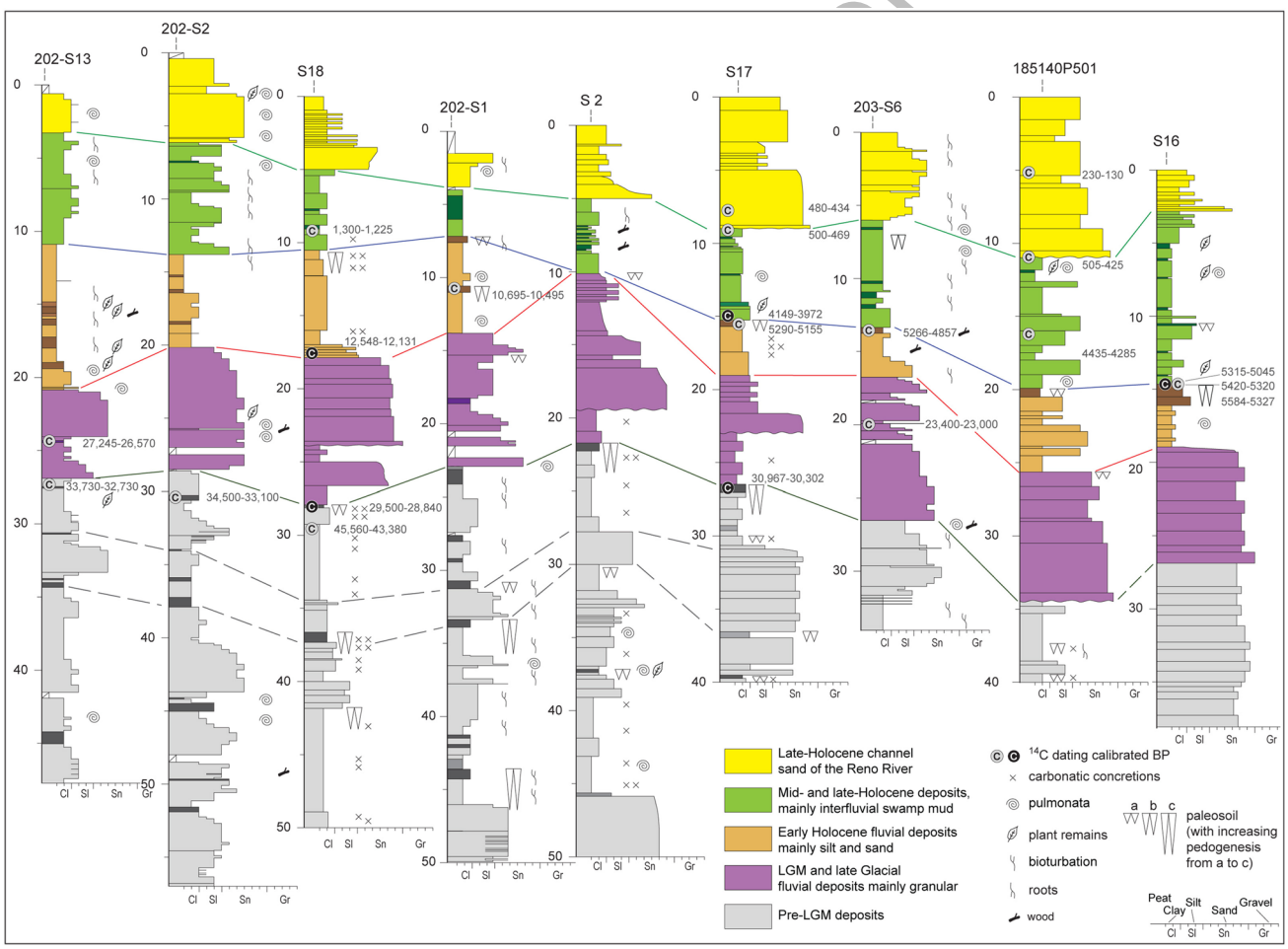

Fig. 5 Stratigraphic correlation of nine subsurface cores, associated with calibrated ^{14}C dating and arranged according to their geographic position and present-day elevation. The geographic location of cores is represented in Fig. 2 by squared symbols. The depositional units accumulated through late Pleistocene and Holocene times and record syndepositional vertical displacement. Correlation lines are traced with the same colour code used in Figs. 7 and 8. The regional framework of the subsurface stratigraphic units is illustrated by Figs. 7 and 8

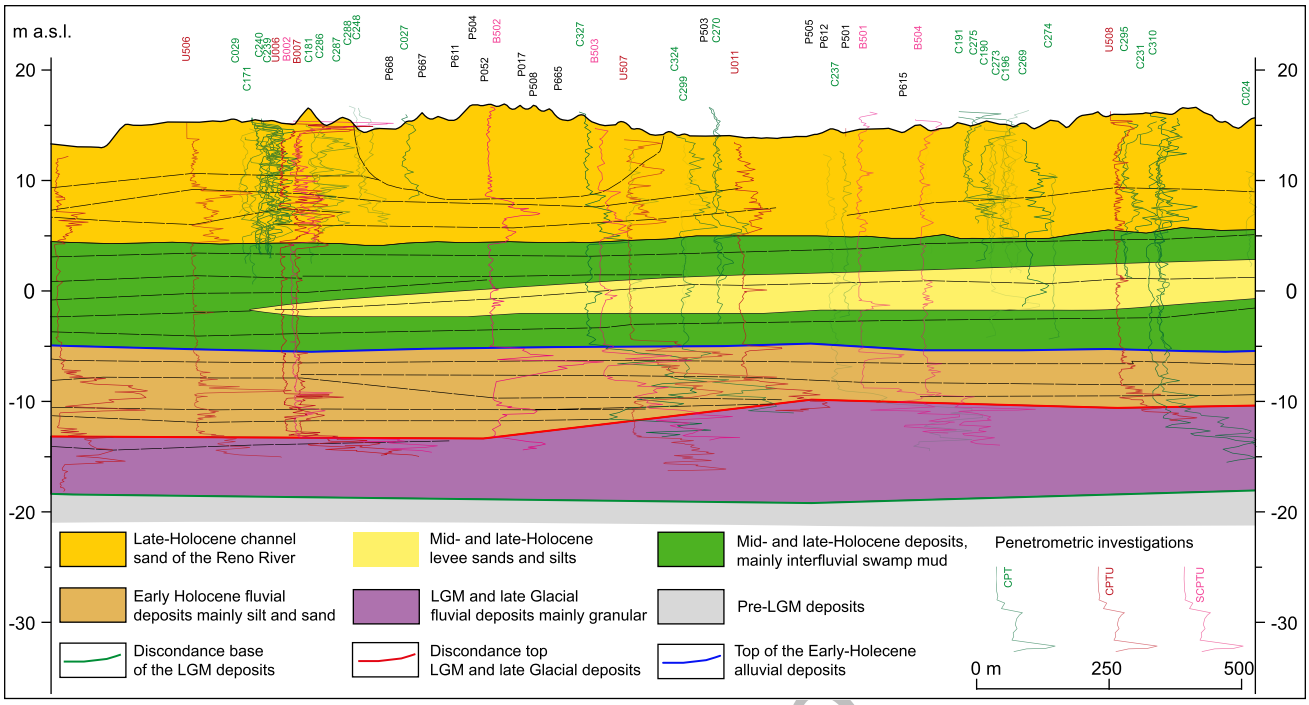

Fig. 6 Example of the high-resolution correlation of cone penetration tests in a small portion of the continuous profile A–A′ (Fig. 7). Geographic location is depicted by the brace symbol in Fig. 4

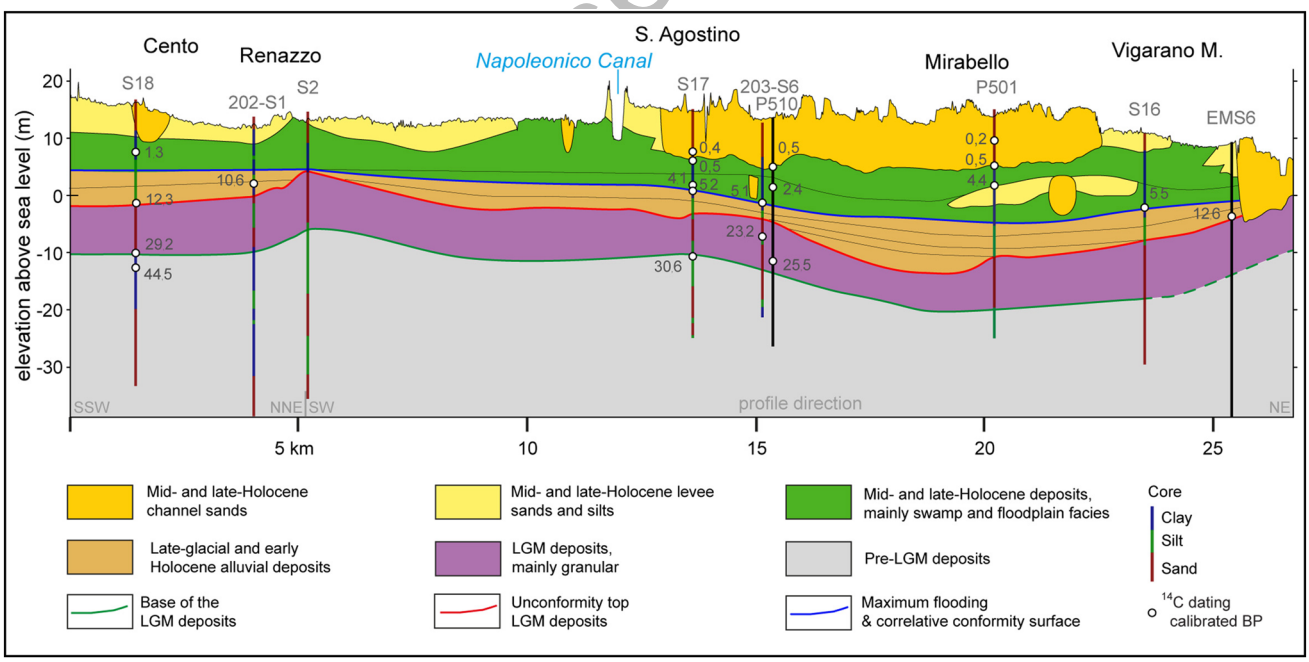

Fig. 7 Detailed stratigraphic profile A–A′, in the central-northern portion of the study region (location in Figs. 2, 4), based on the methodology illustrated by Fig. 6. Numbers indicate calibrated ^{14}C dating expressed in thousands of years BP. The profile provides the best evidence for the estimation of the vertical displacements of the stratigraphic units and surfaces. A large post-depositional deformation is clearly visible

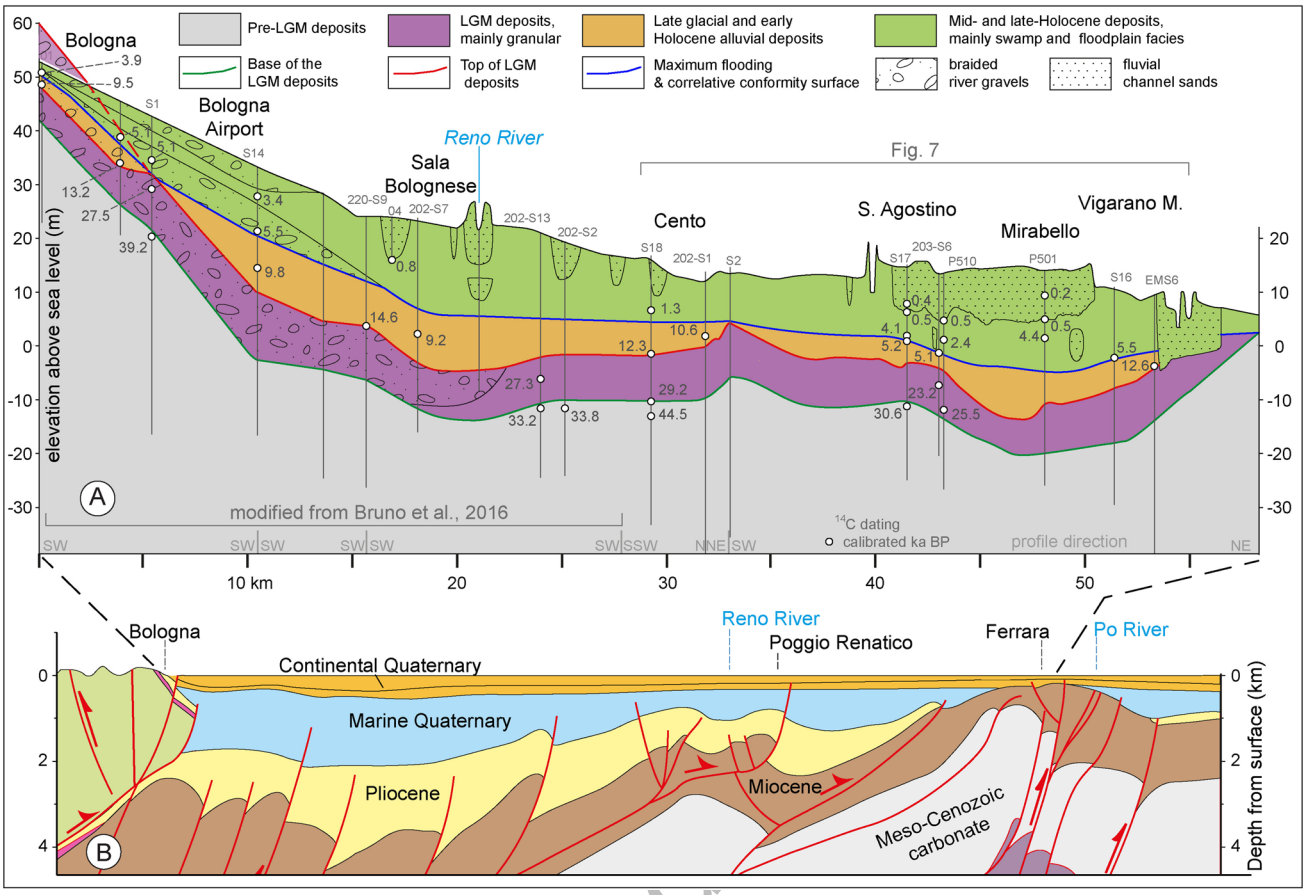

Fig. 8 Regional stratigraphic profile B–B′ (location in Figs. 1, 2) elongated from the Apennines foothills, near Bologna, to the Po deposits, near Ferrara. Numbers indicate calibrated ^{14}C dating in thousands of years BP. The lower portion provides a synthetic view of the underlying tectonic elements (cf. Fig. 4). The large deformation affecting the sedimentary unit is clearly visible and is spatially correlated with the underlying tectonic structures

Sediments predating the Last Glacial Maximum

The young Pleistocene unit (Pre-LGM, Fig. 5) belongs to the upper portion of the AES7 Villa Verrucchio Subsynthem (Molinari and Pizziolo 2009). In northern areas, the interval consists of coarse fluvial sand (e.g. Core S18 at Vigarano Mainarda, Figs. 5, 7), recording a Po River input (Cibin and Segadelli 2009). In the central-southern portion of the profile A–A′ area (Mirabello and Cento, Fig. 2), the unit is rich in silt and clay sediments, encompassing elongated river sand bodies, generally 2–3 m thick, recording a provenance from the Apennines (Albertini et al. 2009; Bruno et al. 2015).

In the southern portion of the profile B–B′, the unit mainly consists of coarse grained, gravel sediments. The regional morphology dipped toward the Po River drainage axis. The occurrence of a cold climate phase is suggested by pollen assemblages (Core 220-S3, Martelli et al. 2009b) and by the finding of mammals adapted to those conditions (e.g., *Bison priscus, Coelodonta antiquitatis, Mammuthus primigenius, Megaloceros giganteus*, Sala and Gallini 2002). The unit top, when not eroded, is marked by a widespread soil level (e.g., Cores S18, S17, 202-S02, Figs. 5, 7), characterized by the occurrence of B or B/C horizons, with carbonate concretions up to 2 cm, and Fe–Mn nodules of 1–2 mm.

Chronological data

In the profile A–A′, we dated the organic horizon of the soil marking the unit top to 31 and 29 ka BP (Cores S17 and S18, Figs. 5, 7, Table 1). In the southern part of the study area, the unit top is also frequently dated at between 30 and 29 ka BP (e.g. cores 220-0S4, Martelli et al. 2009b, 202-S1; Molinari and Pizziolo 2009), but other samples provided younger ages, between 29 and 27 ka BP (Amorosi et al. 2016a). In the southernmost portion of the region, the unit top layer provided older ages of about 33 ka (202-S2, 202-S13, Molinari and Pizziolo 2009; Amorosi et al. 2016a, Figs. 5, 8), or even 39 ka BP (Bruno et al. 2015). Within the profile A–A′, samples from lower levels were dated to older ages,

in good agreement with their stratigraphic position (44.5 ka BP S18, Amorosi et al. 2016a). At a site near the northern termination of the profile, our calibration of the previous ^{14}C measurements on bones from the unit (Sala and Gallini 2002) produced ages of 34–40 ka BP.

Environmental interpretation

The pre-glacial unit records middle alluvial plain environments, with wide braided river channels developed under relatively cold climate conditions. During the MIS 3 stage, the mouth of Po River was positioned well to the south of the modern one (Correggiari et al. 1996) and the rivers outflowing the Apennines were all tributary of the Po River, toward which the topographic surface dipped. The unit top experienced a comparatively long exposure, allowing the formation of a multiphase palaeosol (Amorosi et al. 2014, 2016a; Bruno et al. 2015, 2016), associated with a stratigraphic gap.

Last glacial maximum and late glacial sediments

The glacial unit (LGM, Figs. 5, 7, 8) is dominated by coarse granular sediments, forming the uppermost part of the AES7 Villa Verrucchio Subsynthem. The base of the unit is normally sharp, being emphasized by the previously described palaeosol and by a widespread increase in grain size. The unit top is also sharp and marked by a new regional soil layer, commonly followed by finer grained sediments. In the northern portion of the profile A–A′ (Fig. 7), the unit consists of medium-coarse grained sand with rare silt layers, organized into amalgamated channel sand bodies, recording a Po River input (Campo et al. 2016). North of Mirabello (Figs. 2, 7), a transition to fine-grained sands (Cores 202-S01, S2014, S17, 203-S6, Figs. 5, 7) of Apennine provenance occurs (Cibin and Segadelli 2009). At the town of Cento (Fig. 2), we sampled from the unit (Log S18, Fig. 5) sub-centimetre limestone and chert clasts, recording a provenance from Ligurian formations of the Apennines. In the southern portion of the B–B′ profile, the unit consists of gravelly sands, grading southward into coarse gravel, also recording a provenance form the Apennines (Albertini et al. 2009; Marchesini et al. 2000; Molinari and Pizziolo 2009). Pollens are scanty in the coarse grained unit. At the northwest of Bologna, herbaceous and *Pinus* pollens were, however, found, suggesting cold periglacial environments (Core 220-S3, Bassetti in Martelli et al. 2009b).

Chronological data

The paucity of organic material often prevents the unit from being directly dated by radiocarbon measurement. Near Ferrara, a sample from the basal portion of the unit was dated at 27 ka BP (Amorosi et al. 2016a). In the area crossed by the profile A–A′, a few fine-grained beds were dated at about 25 and 23 ka BP (Cores 203-S6, P510, Cibin and Segadelli 2009). In the southern part of the study region, samples from the lower portion of the unit were dated at 27 and 26 ka BP (Log 201-S13, Gasperi and Pizziolo 2009, Figs. 5, 7). In the Bologna urban area, several organic-rich clays sampled from the interval were dated at between 26 and 20 ka BP (26 ka 221-S12, 24 ka 221-S4, 22 ka 221-S1, 20 ka 221-S5, 20 ka 221-S11, Martelli et al. 2009a). At the north-west of Bologna, a level near the top of the unit provided an age of 14.5 ka BP (Martelli et al. 2009a). The organic-rich soil level marking the top of the unit provided ages of 12.6 and 12.3 ka BP (Cores EMS6 and S18, respectively). We dated a pine cone from the very top of the unit (strobilus of *Pinus* from core S18, Figs. 5, 7) at 12.5 ka BP (Table 1). Seven dating of the top soil level in the Bologna urban area generated ages between 12.9 and 11.5 ka BP (Amorosi et al. 2016a; Bruno et al. 2015), demonstrating that the soil developed during the Younger Dryas climate phase.

Environmental interpretation

The unit was formed by braided rivers, supplied by Apennine streams and, in the northern area, by the Po River. The middle-lower part of the unit accumulated during the climax of the LGM and the beginning of the deglaciation, between 24 and 16 ka BP. The interval sedimented during the LGM marine lowstand and the early phase of the following marine transgression, when the study area was distant from the coastline and all the rivers outflowing the Northern Apennines were tributaries of the Po (Correggiari et al. 1996; Stefani and Vincenzi 2005; Amorosi et al. 2016a). The depositional morphology dipped toward the Po River axis and was smoothed out by the active braided river divagation and aggradation. The top portion of the unit formed during the Late Glacial times, when Alpine glaciers withdrawn into the high sector of the mountain catchments, and many Alpine valleys were blocked by large lakes. These factors strongly limited the sedimentary input from the Alps, inducing the entrenchment of the Alpine tributaries of the Po and the interruption of the sedimentation over large sectors of the plain, at the north of this river (Fontana et al. 2014). Terrace development was recognized in the subsurface of the modern coastal area (Stefani and Vincenzi 2005; Cibin and Stefani 2009) and near Ferrara (Amorosi et al. 2016a). The main streams fed by the Apennines experienced a reduction of the sedimentary input, which, however, remained active until the Younger Dryas climate phase (Amorosi et al. 2016a).

Lower Holocene sediments

The unit (Post-LGM1, Figs. 5, 7, 8) is dominated by silt and silty clay sediments, grading upward into organic-rich clay

and peat, with subordinated fluvial sands. Weakly developed soils are found in the lower portion of the unit, but they become sparser further up, while organic-rich layers increase in frequency. The early Holocene interval forms the lower portion of the AES8 Ravenna Subsynthem. The base corresponds to the previously described palaeosol, associated with a variable stratigraphic gap. The top of the unit corresponds to a widespread organic-rich clay horizon.

In northern areas, Po River sands were deposited. In the central-southern portion of the profile A–A′ region, the unit is dominated by large volumes of brown silt or silty clay, deposited into interfluvial areas, associated with fluvial channel sand, recording a provenance form the Apennines (Martelli et al. 2009b). Silt and silty clay sediments are also common in the southern portion of the profile B–B′ and record a fining upward evolution. Coarser grained lithologies are documented only near the Apennines. Gravel units are confined to incised valley settings, at the apex of the fluvial fans (Martelli et al. 2009b; Molinari and Pizziolo 2009).

Chronological data

A diachronous onset of the unit deposition is suggested by the onlap relationship inferred at its base (Fig. 7) and by the results of the ^{14}C dating. At the north-west of the profile termination, near Ferrara (Fig. 1), a peat level from the unit was dated at 7.3 ka BP (Core 185P505, Campo et al. 2016). In the central portion of the profile A–A′, a soil from the lower portion of the unit is dated at about 10.6 ka BP (Core 202-S01, Molinari and Pizziolo 2009, Figs. 5, 7). The area between Sala Bolognese and the Bologna Airport (Fig. 8) provided ages between 9.8 and 9.2 ka BP (Martelli et al. 2009b). In the southernmost portion of the study area, a sample was dated at 9.5 ka BP (Bruno et al. 2016, Fig. 8). The dating of the organic-rich horizons marking the unit top produced a tight cluster of ages at around 5.5–5.0 ka BP (e.g., Cores S17 203-S6, S16, Cibin and Segadelli 2009, Fig. 5), suggesting a fairly synchronous development of the top portion of the unit.

Environmental interpretation

The diachronous starting of the unit deposition is associated with a widespread time gap and with the development of a mature soil. In the study region, this phase is the only one, through the last 45,000 years, when non-deposition prevailed over sedimentation. The unit records an evolution from braided rivers to lower alluvial plain systems, grading eastward into delta-estuarine environments. The evolution was associated with the transgression of the Adriatic Sea, driven by the eustatic rise (Correggiari et al. 1996; Lambeck et al. 2004; Amorosi et al. 2016b). In northern portions of the study area, the Po River initially developed meandering systems, reworking glacial sand, and then evolved through the formation of fluvial ridges. In the central portion of the region, fluvial sedimentation restarted in the topographically depressed areas, fed by Apennine-derived rivers, which were temporarily prevented from directly reaching the Po drainage axis. The topographic lower areas correspond to synclines structures, as in the Mirabello region (profile A–A′, Fig. 7). Fluvial sedimentation then spread out, generating an onlap relationship on the previous topographic surface (Fig. 7). The depositional environment was initially characterized by well-drained interfluvial areas, subject to pedogenesis, which evolved into moist interfluvial depressions, particularly in areas corresponding to syncline structures. At the ending time of the unit deposition, sedimentation had spread out throughout the study region and the topographic gradients were reduced. The unit top correlates with the maximum flooding phase (Correggiari et al. 1996; Amorosi et al. 2016b), when the Adriatic Sea reached a coastline about 60 km from the study area (Stefani and Vincenzi 2005). At the time, the reduced topography gradients were dipping toward the Po River channels and estuary mouths.

Upper Holocene sediments

The unit (Post-LGM2, Figs. 5, 7, 8) is dominated by large volumes of argillaceous sediments, with subordinated fluvial channel sand. The base of the interval corresponds to the concordant top of the underlying unit. The top corresponds to the present-day topography. In the northernmost portion of the profile, the unit records wide channels of the Po. In the central-southern area of the profile A–A′, the interval mainly consists of argillaceous sediments, lacking evidence of significant pedogenesis.

In the southern portion of the B–B′ profile, the unit is dominated by fine-grained sediments, with some elongated sand bodies deposited by the Reno River and other Apennine streams. Coarse gravelly sands and gravels accumulated only near the Apennine foothills, mainly into incised valley setting (Martelli et al. 2009b; Molinari and Pizziolo 2009).

Chronological data

Peat horizons from the lower portion of the unit are generally dated at between 5 and 4 ka BP (cores S17, 185140P501, Figs. 5, 7, Table 1), but near Cento a much younger age of 1.2 ka BP was measured from the lower part of it (Amorosi et al. 2016a, Figs. 5, 7). Both historic information and radiometric dating demonstrate that the thick fluvial body forming the upper portion of the profile A–A′ (Fig. 7) was deposited by the Reno River, between the 16th and 18th centuries AD.

Environmental interpretation

Through the majority of the study area, the unit accumulated into distal alluvial plain systems. The fluvial channels were generally elevated and hanging on the surrounding depressions. The Apennine rivers were often tributary of the Po. Coarser grained sediments are confined to near piedmont settings. Through the last three millennia, a growing degree of human intervention influenced the depositional evolution. During the last two centuries, the hydrographic network of the study region became almost completely artificial in nature.

Vertical displacement, impact, and amount

Lateral variation of the stratigraphic thickness

The thickness of the *Glacial unit* (LGM, violet unit, Fig. 8) climaxes at 18 m, in the foot-hill belt, is 13 m in the southern syncline area (Fig. 8), and thins out to 6 m, in the middle anticline belt (north of Cento). In the northern syncline depression, the unit develops a thickness between 10 and 12 m (Mirabello), and then thins out northward (Figs. 2, 7), to disappear altogether, in the external anticline area (Fig. 2).

The thickness of the *lower Holocene unit* (brown, Fig. 8) climaxes at 12 m, in the southern structural depression (Sala Bolognese), and at 9.5 m in the northern one (Mirabello, Figs. 2, 7). The interval thins out to zero in three areas: along the Apennines foothill belt, on the central structural high (Renazzo), and in the anticline belt at the north-west of Ferrara (Minarelli 2013).

The *upper Holocene unit* (green unit, Fig. 8) ranges in thickness from zero, near the Apennines foothill, to more than 22 m, in the southern syncline area (Sala Bolognese). The unit thins out to 6–7 m on the central anticline belt (Cento-Renazzo), thickens to 20 m in the northern syncline area (south of Mirabello), and then thins to 3–4 m, on the external anticline culmination.

Present-day elevation and dip of the stratigraphic surfaces

The importance of the post-depositional movements shows up in the depth variation of the stratigraphic surfaces and in the development of southward counterslopes, reversing the primary topography trends. For a correct understanding of the profile B–B′, it is important to remember ("Construction of the stratigraphic panel and regional profiles") that it forms important dihedral angles, varyingly reducing the apparent dip. The angle locations are depicted at the base line of Fig. 8 and correspond to angled changes of the apparent dip.

The *basal surface of the Glacial* unit, near the Apennines foothill, steeply dips toward the alluvial plain, varying in elevation from +42 m above sea level (m.s.l., Casalecchio di Reno), to −2 m below m.s.l., over a distance of about 5 km, with an average dip gradient of 9‰. Further north, the surface descends to −17 m in the southern syncline area (Sala Bolognese), with an actual dip of about 8‰. Northward, the surface climbs to shallower levels, in sharp contrast with its primary topography trend. The base rises from −12 to −6 m, over a distance of just 3 km, on the southern flank of the central anticline high, with an actual southward dip of about 8‰. The unit base descends again northward to −22.5 m, in the core of the northern syncline, with an average dip of about 1‰. The surface rises back to −10 m, at the northern extremity of the profile A–A′, and to +2 m, at the end of the profile B–B′. The northern region shows a counterslope of about 4‰.

The *discordance top surface of the Glacial unit* shows a similar spatial trend of depth variation. The surface is outcropping on the terraced topography near the Apennines, at an elevation between +70 and +60 m (Martelli et al. 2009a, b; Picotti and Pazzaglia 2008; Picotti et al. 2009). The surface steeply descends to +10 m over a distance of 6 km (north of Bologna Airport), with an average dip of 9‰, and then to −5 m, in the southern syncline zone. The surface rises northward to +3 m, in the central anticline area, with an average counterslope of 6‰. The surface descends again northward, reaching −13 m, in the northern syncline zone, and rises back to +2 m, at the end of the profile B–B′.

The *upper boundary of the lower Holocene unit* (post-LGM1) dips northward, in the southernmost part of the profile B–B′, losing about 30 m of elevation over 5 km, with an average gradient of 6‰. The surface descends to +5 m, in the southern syncline area, and stays sub-horizontal, between +6 or +5 m, along a distance of more than 12 km, from the southern syncline to the central anticline area. The surface descends to −4.5 m in the northern syncline zone, and then it rises to +2 m in the external anticline area. The northern area, therefore, shows a gentle southward counterslope, with a dip of less than 1‰.

Measurement of the minimal amount of vertical displacement

It is possible to measure a minimal value of the relative vertical displacement without introducing the uncertainty associated with the reconstruction of the original topographic elevation. This was performed by measuring the elevation of the lowest and highest parts of a stratigraphic surface with respect to a horizontal reference plain, tangential to the highest point of it. In this way, a relative vertical displacement

of the top of the Glacial unit of about − 8 m was measured between the southern syncline and the central anticline area. A displacement of − 18 m was measured between the same anticline and the northern syncline core zone (Fig. 8). For the top surface of the lower Holocene unit, an apparent zero shift was measured across the southern syncline, and one of − 7 m in the northern one. The measured values provide an indication of the order of magnitude of the movement. However, the actual vertical displacement has certainly been greater, since the depositional surfaces were far from being horizontal at the formation time. The surface certainly presented a significant depositional dip toward the main drainage axis provided by the Po River. The palaeotopography was steeper in the area proximal to the Apennines chain, which was richer in coarser grained sediments, than in lower alluvial plain areas near the Po River. These features explain the underestimation of the subsidence in the southern syncline in the previous simplified measurement. A detailed reconstruction of the palaeo-topographic elevation is beyond the aims of our present contribution. However, some preliminary qualitative consideration can be proposed. A subsidence exceeding 20 m, during the last 12,000 years, in both syncline areas, can be suggested. We can preliminary estimate the average rate of the vertical component of deformation by subdividing the displacement affecting a stratigraphic surface by the time interval elapsed since their formation. The starting of the pedogenesis processes marking the top of the Glacial unit is dated to 12.5 ka BP ("Last Glacial Maximum and late Glacial sediments"). The dating generates an estimation of the average subsidence rate of at least − 1.5 m/ka in the syncline areas and of a few decimetres in the anticline sites. The piedmont belt experienced uplift, with an average speed of about 1 m/ka (Picotti et al. 2009).

Discussion

Source of uncertainty in the estimation procedure

The suggested evaluations are subject to various degrees of uncertainty, deriving from the summation of the uncertainties associated with the individual steps of estimation. The knowledge of the present-day topography is excellent thanks to the altimetry data provided by the LIDAR survey. The positioning of the subsurface logs is normally quite good. The stratigraphic correlation within the A–A′ profile is, in our opinion, good, with elevation errors in the magnitude order of a few decimetres. Stratigraphic correlation in other portions of the B–B′ profile is affected by a greater degree of uncertainty, particularly in the southern syncline area, where uncertainty of a few metres locally exists, in the countryside region at the south of Cento, poor in subsurface data ("Construction of the stratigraphic panel and regional profiles"). Considering the primary topography as horizontal is obviously a severe oversimplification, introducing errors of several metres. The magnitude order of displacement is, however, reliable, as it is the geographic trend of the vertical deformation distribution. A good spatial correlation between subsidence trends and the geometry of the buried active tectonic structures is, therefore, certain. The time framework of the study units derived from a large number of ^{14}C measurements performed at different times and at various analytical facilities. We calibrated the entirety of the available measurements in a homogeneous and up to date framework, reducing the heterogeneity of the chronological data set as far as possible. The uncertainty in the chronological estimation is comparatively low and, therefore, a negligible source of error in the estimation procedure of the vertical movement rates.

Factors controlling the stratigraphic thickness distribution

The successions deposited into the more subsiding syncline areas are clearly thicker and record a more continuous sedimentation than those sedimented into anticline sites, which are richer in depositional gaps. A spatial correlation between the thickness distribution and the arrangement of the buried tectonic structures is quite clear (Fig. 8). However, many factors interacted as to shape the present-day thickness of the units. The available accommodation space for sedimentation was influenced by both the local subsidence and the global eustatic fluctuation. The eustasy component was particularly significant during the transgressive evolution, associated with the deposition of the lower Holocene unit, whereas it played a minor role during the Glacial lowstand time and in the recent Holocene interval. The magnitude of the sediment input influenced the aggradational evolution. The availability of Apennine-derived sediment was greater in southern areas than in northern ones. The thickness of the glacial unit was locally affected by some degree of post-depositional erosion, expecially in the piedmont belts and in some anticline settings. No significant erosion, on the contrary, affected the two Holocene units. Post-depositional sediment compaction significantly reduced the thickness of the sedimentary successions, particularly those rich in argillaceous and peat sediments. Compaction evolution is influenced by the burial depth and by the time elapsed since deposition. The late Holocene sediments have, therefore, experienced only a very partial compaction, a factor emphasizing their thickness.

Factors controlling the vertical displacements

The discussed movements derived from the superposition of several components, such as the regional flexural subsidence of the foreland basin, the compressive deformation of the buried tectonic structures, the compaction of the very thick Plio-Pleistocene successions, the migration of subsurface fluids, etc. The thick Quaternary successions are generally very rich in argillaceous sediments and are only incompletely lithified. These features are associated with low seismic velocity values (Minarelli et al. 2016) and with a significant residual compaction potential, which is higher in the thicker successions accumulated into syncline areas than in the much thinner units sedimented into anticline sites. In the northern anticline region, the Pliocene and marine Quaternary sediments are altogether missing and Miocene well-lithified units are found at shallow depth (Figs. 3, 8). Sediment compaction, therefore, plays a major role in the subsidence distribution, emphasizing the subsidence in the syncline areas, characterized by much thicker Plio-Pleistocene successions than the anticline sites (Fig. 2).

The suggested values of vertical displacement are coherent with the average subsidence estimated in the study region through the last 500,000 years on the base of the subsurface stratigraphy reconstruction (cf. Regione Emilia Romagna ENI 1998; Minarelli et al. 2016). An average subsidence rate of about 1.5 m/ka in the syncline area was, in this way, estimated. This value is about half of those recently measured in the syncline areas (Bondesan et al. 1997, 2000; ARPA 2012; Martelli et al. 2017). The comparison suggests that the anthropic alteration is presently playing a major role in accelerating the subsidence, at the regional scale (Cenni et al. 2013).

Conclusions

(a) The collection, GIS organization, and stratigraphic correlation of a large number of cores and cone penetration tests, calibrated by new stratigraphic coring and ^{14}C dating, has demonstrated itself as a valuable and cost-effective tool to understand unlithified sediments.

(b) The units deposited through the last 45,000 years onto the buried structures of the Apennines show important lateral variations in thickness. The successions accumulated into syncline sites are much thicker than their anticline counterparts.

(c) A large amount of post-depositional vertical displacement affects the study late Quaternary successions. We estimated that the stratigraphic surfaces formed at 12.5 and 5 ka BP subsided for up to at least − 18 and − 7 m, respectively, in the syncline areas. Subsidence rate in syncline sites exceeded 1.5 m/ka.

(d) The lateral gradient of subsidence influenced the depositional evolution, which was also controlled by the large eustatic and climatic fluctuations. The environmental expression of the subsidence gradient changed through time. In periods of sediment paucity, such as during the post-glacial depositional gap time, deformation was able to generate a topographic denivelation, directly impacting on the fluvial drainage evolution. During intervals of fast sedimentation, the palaeotopography was smoothed and the drainage framework was less influenced by the subsidence gradient. Spatial gradients of subsidence were, however, always able to exert some degree of influence on the development of the fluvial drainage network.

(e) The suggested measures of the vertical displacement can support future modelling attempt of the subsidence dynamics. The original data provided by the research will help an improved understanding of the genetic factors of deformation, in the Apennines Foreland Basin and in other similar ancient and modern basin worldwide.

Acknowledgements We thank Daniel Egli and Christoph Grützner for their accurate and helpful reviews, and Riccardo Caputo and Daniela Fontana for critical discussion. We thank the Servizio Geologico, Sismico e dei Suoli della Regione Emilia Romagna and the Municipal Administration of Ferrara for the access to the subsurface data bases and for financial support in early stages of the research. A part of the subsurface data gathering and preliminary interpretation was carried out within a seismic risk microzonation project for the municipalities of Cento, Mirabello, Sant'Agostino, and Sala Bolognese. This research did not receive any specific grant from funding agencies in the public, commercial, or not-for-profit sectors.

References

Albertini C, Ceriani A, Di Giulio A (2009) Petrografia delle sabbie di sottosuolo. In: Molinari FC, Pizziolo M (eds, Note illustrative della carta Geologica d'Italia alla scala 1:50,000. Foglio 202 San Giovanni in Persiceto, pp 87–97

Alessio G, Alfonsi L, Brunori CA, Burrato P, Casula G, Cinti FR, Civico R, Colini L, Cucci L, De Martini PM, Falcucci E, Galadini F, Gaudiosi G, Gori S, Mariucci MT, Montone P, Moro M, Nappi R, Nardi A, Nave R, Pantosti D, Patera N, Pesci A, Pezzo G, Pignone M, Pinzi S, Pucci S, Salvi S, Tolomei C, Vannoli P, Venuti A, Villani F (2013) Liquefaction phenomena associated with the Emilia earthquake sequence of May–June 2012 (Northern Italy). Nat Hazards Earth Syst Sci 13:935–947. https://doi.org/10.5194/nhess-13-935-2013

Amorosi A, Marchi N (1999) High-resolution sequence stratigraphy from piezocone tests: an example from the Late Quaternary deposits of the SE Po Plain. Sediment Geol 128:69–83. https://doi.org/10.1111/bre.12174

Amorosi A, Severi P (2009) Note Illustrative della Carta Geologia d'Italia alla scala 1:50,000, Foglio 221, Bologna, Settore di pianura. Servizio Geologico d'Italia, p 107

Amorosi A, Colalongo ML, Fusco F, Pasini G, Fiorini F (1999) Glacio-eustatic control of continental-shallow marine cyclicity from Late Quaternary deposits of the south-eastern Po Plain (Northern Italy). Quatern Res 52:1–13

Amorosi A, Bruno L, Rossi V, Severi P, Hajdas I (2014) Paleosol architecture of a late Quaternary basin-margin sequence and its implications for high resolution, non-marine sequence stratigraphy. Glob Planet Change 112:2–2. https://doi.org/10.1016/j.gloplacha.2013.10.007

Amorosi A, Bruno L, Cleveland DM, Morelli A, Wan H (2016a) Paleosols and associated channel-belt sand bodies from a continuously subsiding late Quaternary system (Po Basin, Italy): new insights into continental sequence stratigraphy. Geol Soc Am Bull 129(3–4):449–463. https://doi.org/10.1130/B31575.1

Amorosi A, Enrico D, Veronica RS, Vaiani M. Sacchetto (2016b) Late Quaternary palaeoenvironmental evolution of the Adriatic coastal plain and the onset of Po River Delta. Palaeogeogr Palaeoclimatol Palaeoecol 268:80–90. https://doi.org/10.1016/j.palaeo.2008.07.009

ARPA (2012) Rilievo della subsidenza nella pianura Emiliano-Romagnola. http://www.arpa.emr.it/index.asp?idlivello=1414

Basili R, Valensise G, Vannoli P, Burrato P, Fracassi U, Mariano S, Tiberti MM, Boschi E (2008) The Database of Individual Seismogenic Sources (DISS), Version 3: summarizing 20 years of research on Italy's earthquake geology. Tectonophysics 453:20–43. https://doi.org/10.1016/j.tecto.2007.04.014

Bignami C, Burrato P, Cannelli V, Chini M, Falcucci E, Ferretti A, Gori S, Kyriakopoulos C, Melini D, Moro M, Novali F, Saroli M, Stramondo S, Valensise G, Vannoli P (2012) Coseismic deformation pattern of the Emilia 2012 seismic sequence imaged by Radarsat-1 interferometry. Ann Geophys 55 4:788–795

Boccaletti M, Bonini M, Corti G, Gasperini P, Martelli L, Piccardi L, Severi P, Vannucci G (2004) Cart asismotettonica della Regione Emilia-Romagna, scala 1:250,000. Con note illustrative. Regione Emilia-Romagna-SGSS, CNR-IGG, SELCA

Boccaletti M, Corti G, Martelli L (2011) Recent and active tectonics of the external zone of the Northern Apennines (Italy). Int J Earth Sci 100:1331–1348. https://doi.org/10.1007/s00531-010-0545-y

Bondesan M, Gatti M, Russo P (1997) Movimenti verticali del suolo nella Pianura Padana orientale desumibili dai dati I.G.M. fino a tutto il 1990. Bollettino di Geodesia e scienze affini 2:141–172

Bondesan M, Gatti M, Russo P (2000) Subsidence in the eastern Po Plain (Italy). Land Subsid 3:193–204

Bronk Ramsey C (2009) Bayesian analysis of radiocarbon dates. Radiocarbon 51(3):337–360. https://doi.org/10.2458/azu_js_rc.51.3494

Bruno L, Amorosi A, Severi P, Bartolomei P (2015) High-frequency depositional cycles within the late Quaternary alluvial succession of Reno River (northern Italy). Ital J Geosci 134(2):339–354. https://doi.org/10.3301/IJG.2014.4

Bruno L, Amorosi A, Severi P, Bianca C (2016) Late Quaternary aggradation rates and stratigraphic architecture of the southern Po Plain, Italy. 2016. Basin Res 29:1–15. https://doi.org/10.1111/bre.12174

Campo B, Amorosi A, Bruno L (2016) Contrasting alluvial architecture of Late Pleistocene and Holocene deposits along a 120-km transect from the central Po Plain (northern Italy). Sediment Geol 341:265–275. https://doi.org/10.1016/j.sedgeo.2016.04.013

Caputo R, Iordanidou K, Minarelli L, Papathanassiou G, Poli ME, Rapti-Caputo D, Sboras S, Stefani M, Zanferrari A (2012) Geological evidence of pre-2012 seismic events, Emilia Romagna, Italy. Ann Geophys 4:743–749. https://doi.org/10.4401/ag-6148

Caputo R, Pellegrinelli A, Bignami C, Bondesan A, Mantovani A, Stramondod S, Russo P (2014) High-precision levelling, DInSAR and geomorphological effects in the Emilia 2012 epicentral area. Geomorphology2 235:106–117. https://doi.org/10.1016/j.geomorph.2015.02.002

Caputo R, Poli ME, Minarelli L, Rapti D, Sboras S, Stefani M, Zanferrari A (2016) Palaeoseismological evidence for the 1570 Ferrara earthquake, Italy. Tectonics 35(2):1423–1445. https://doi.org/10.1002/2016TC004238

Carminati E, Doglioni C, Scrocca D (2005) Magnitude and causes of long-term subsidence of the Po Plain and Venetian region. In: Flecker CA, Spencer T (eds) Flooding and environmental challenges for Venice and its lagoon: state of knowledge. Cambridge University Press, Cambridge, pp 21–28

Castiglioni GB, Ajassa R, Baroni C, Biancotti A, Bondesan A, Bondesan M, Brancucci G, Castaldini D, Castellaccio E, Cavallin A, Cortemiglia F, Cortemiglia GC, Cremaschi M, Da Rold O, Elmi C, Favero V, Ferri R, Gandini F, Gasperi G, Giorgi G, Marchetti G, Marchetti M, Marocco R, Meneghel M, Motta M, Nesci O, Orombelli G, Paronuzzi P, Pellegrini GB, Pellegrini L, Rigoni A, Sommaruga M, Sorbini L, Tellini C, Turrini MC, Vaia F, Vercesi PL, Zecchi R, Zorzin R (1997) Geomorphological map of the Po Plain. 3 Sheets at 1:250,000 scale. SELCA, Firenze

Cenni N, Viti M, Baldi P, Mantovani E, Bacchetti M, Vannucchi A (2013) Present vertical movements in central and northern Italy from GPS data: possible role of natural and anthropogenic causes. J Geodyn 71:74–85

Cibin U, Segadelli S (2009) Note Illustrative della Carta Geologia d'Italia alla scala 1:50,000, Foglio 203, Poggio Renatico. Servizio Geologico d'Italia, Rome, p 104

Cibin U, Stefani M (2009) Note Illustrative della Carta Geologia d'Italia alla scala 1:50,000. Foglio 187, Codigoro. Servizio Geologico d'Italia, Rome, p 162

Clark P, Dyke A, Shakun J, Carlson A, Clark J, Wohlfarth B, Mitrovica J, Hostetler S, McCabe A (2009) The Last Glacial Maximum. Science 325:710–714. https://doi.org/10.1126/science.1172873

Correggiari A, Roveri M, Trincardi F (1996) Late Pleistocene and Holocene evolution of the North Adriatic Sea. Ital J Quatern Sci 9:697–704

De Mio G, Giacheti HL (2007) The use of piezocone tests for high-resolution stratigraphy of Quaternary Sediment Sequences in the Brazilian coast. Ann Braz Acad Sci 79(1):153–170. https://doi.org/10.1590/S0001-37652007000100017

DISS Working Group (2015): Database of Individual Seismogenic Sources (DISS), version 3.2.0: a compilation of potential sources for earthquakes larger than M 5.5 in Italy and surrounding areas. Istituto Nazionale di Geofisica e Vulcanologia. https://doi.org/10.6092/INGV.IT-DISS3.2.0. http://diss.rm.ingv.it/diss/

FAO-ISRIC (2006) Guidelines for soil description, 4th edn. International Soil Reference Information Centre, Rome, p 97

Fontana A, Mozzi P, Marchetti M (2014) Alluvial fans and megafans along the southern side of the Alps. Sediment Geol 301:150–171. https://doi.org/10.1016/j.sedgeo.2013.09.003

Galli P, Castenetto S, Peronace E (2012) The MCS macroseismic survey of the 2012 Emilia earthquakes. Ann Geophys 55(4):663–672. https://doi.org/10.4401/ag-6163

Gasperi G, Pizziolo M (2009) Note Illustrative della Carta Geologia d'Italia alla scala 1:50,000. Foglio 201, Modena. Servizio Geologico d'Italia, Rome, p 76

Ghielmi M, Minervini M, Nini C, Rogledi S, Rossi M, Vignolo S (2010) Sedimentary and tectonic evolution in the eastern Po-Plain and northern Adriatic Sea area from Messinian to Middle Pleistocene (Italy). Rendiconti Lincei 21(Suppl):131–166

Guidoboni E (1987) I terremoti del territorio ferrarese. In: Bocchi F (ed) Storia di Ferrara AIEP 40:625–640

Guidoboni E, Ferrari G, Mariotti D, Comastri A, Tarabusi G, Valensise G (2007) Catalogue of Strong Earthquakes in Italy from 461 B.C. to 1997 and in the Mediterranean area, from 760 B.C. to 1500.

An Advanced Laboratory of Historical Seismology. http://storing.ingv.it/cfti4med/

Lambeck, K, Rouby H, Purcell A, Sun Y, Sambridge M (2004) Sea level and global ice volumes from the Last Glacial Maximum to the Holocene. Proc Natl Acad Sci USA 111(43):15296–15303. https://doi.org/10.1073/pnas.1411762111

Marchesini L, Amorosi A, Cibin U, Zuffa G, Spadafora E, Preti D (2000) Sand composition and sedimentary evolution of a Late Quaternary depositional sequence, North-western Adriatic coast, Italy. J Sediment Res 70(4):829–838. https://doi.org/10.1306/2DC4093B-0E47-11D7-8643000102C1865D

Martelli L, Amorosi A, Severi P (2009a) Note Illustrative della Carta Geologica d'Italia, Foglio 221, Bologna. Regione Emilia Romagna e APAT, scala 1:50,000, Servizio Geologico, Sismico e dei Suoli, Regione Emilia Romagna. System Cart S.r.l Roma, p 108

Martelli L, Benini A, De Nardo MT, Severi P (2009b) Note Illustrative della Carta Geologica d'Italia, Foglio 220, Casalecchio di Reno. Regione Emilia Romagna e APAT, scala 1:50,000, Servizio Geologico, Sismico e dei Suoli. Regione Emilia Romagna, System Cart S.r.l, Rome, p 124

Martelli L, Bonini M, Calabrese L, Conti G, Ercolessi G, Molinari FC, Piccardi L, Pondrelli S, Sani F, Severi P (2017) Note illustrative della carta sismo tettonica della Regione Emilia-Romagna ed aree limitrofe. Regione Emilia-Romagna, Servizio Geologico, p 93

Michetti AM, Giardina F, Livio F, Mueller K, Serva L, Sileo G, Vittori E, Devoti R, Riguzz F, Carcano C, Rogledi S, Bonadeo L, Brunamonte F, Fioraso G (2012) Active compressional tectonics, Quaternary capable faults, and the seismic landscape of the Po Plain (northern Italy). Ann Geophys 55:969–1001. https://doi.org/10.4401/ag-5462

Minarelli L (2013) Ricostruzione geologica tridimensionale della stratigrafia tardo-quaternaria nel sottosuolo di Ferrara. Università di Ferrara. Tesi di Dottorato GEO/02. http://eprints.unife.it/805/1/Tesi%20Dottorato%20Minarelli.pdf, p 247

Minarelli L, Amoroso S, Tarabusi G, Stefani M, Pulelli G (2016) Down-hole geophysical characterization of middle-upper Quaternary sequences in the Apennine Foredeep, Mirabello, Italy. Ann Geophys 59(5):1–8

Molinari FC, Pizziolo M (2009) Note Illustrative della Carta Geologia d'Italia alla scala 1:50,000, Foglio 202, San Giovanni in Persiceto. Servizio Geologico d'Italia, p 104

Pezzo G, Merryman Boncori JP, Tolomei C, Salvi S, Atzori S, Antonioli A, Trasatti E, Novali F, Serpelloni E, Candela L, Giuliani R (2013) Coseismic deformation and source modeling of the May 2012 Emilia (Northern Italy) earthquakes. Seismol Res Lett 84(4):645–655. https://doi.org/10.1785/0220120171

Picotti V, Pazzaglia FJ (2008) A new active tectonic model for the construction of the Northern Apennines mountain front near Bologna (Italy). J Geophys Res 113:1–24

Picotti V, Ponza A, Pazzaglia FJ (2009) Topographic expression of active faults in the foothills of the Northern Apennines. Tectonophysics 474:285–294

Pieri M, Groppi G (1981) Subsurface geological structure of the Po Plain, Italy. Consiglio Nazionale delle Ricerche, Progetto finalizzato Geodinamica, Sottoprogetto Modello Strutturale, Pubbl.414, PF Geodinamica. C.N.R, p 23

Pizzi A, Scisciani V (2012) The May 2012 Emilia (Italy) earthquakes: preliminary interpretations on the seismogenic source and the origin of the coseismic ground effects. Ann Geophys 55(4):751–757. https://doi.org/10.4401/ag-6171.1

Pondrelli S, Salimbeni S, Perfetti P, Danecek P (2012) Quick regional centroid moment tensor solutions for the Emilia 2012 (northern Italy) seismic sequence. Ann Geophys 55(4):615–621. https://doi.org/10.4401/ag-6146

QUEST (2012): Rapporto macrosismico sui terremoti del 20 (ML 5.9) e del 29 maggio 2012 (ML 5.8 e 5.3) nella pianura padano-emiliana. Gruppo di lavoro INGV Roma e INGV Bologna. http://quest.ingv.it/images/quest/QUEST_Emilia2012_

Regione Emilia-Romagna (1999) Carta geologica di pianura dell'Emilia-Romagna. A cura di D. Preti. Regione Emilia-Romagna. Servizio Sistemi Informativi Geografici, ufficio geologico. S.EL.CA., Firenze

Regione Emilia-Romagna (2012) Sisma 2012: Studi sismici e cartografia di riferimento. http://ambiente.regione.emilia1465omagna.it/geologia/temi/sismica/speciale-terremoto/sisma-2012-ordinanza-70-13-11-2012-cartografia

Reimer P, Bard E, Bayliss A, Beck J, Blackwell P, Ramesy C, Van der Plicht J (2013) IntCal13 and Marine13 radiocarbon age calibration curves 0–50,000 years cal BP. Radiocarbon 55(4):1869–1887. https://doi.org/10.2458/azu_js_rc.55.16947

RER-ENI, Agip (1998) Riserve idriche sotterranee della Regione Emilia-Romagna. A cura di G. M. Di Dio. Regione Emilia-Romagna, ENI Agip Divisione Esplorazione e Produzione. S.EL.CA., Firenze, p 120

Sala B, Gallini V (2002) La steppa-taiga a mammut e rinoceronti lanosi di Settepolesini—Il popolamento faunistico e gli ambienti di pianura durante l'Ultimo Glaciale. AAVV "Studi di geomorfologia, zoologia e paleontologia nel Ferrarese". Accademia delle Scienze di Ferrara e Società Naturalisti Ferraresi, Ferrara, pp 39–45

Sanesi G (ed) (1977) Guida alla descrizione del Suolo. CNR, Firenze, p 113

Saraò A, Peruzza L (2012) Fault-plane solutions from moment-tensor inversion and preliminary Coulomb stress analysis for the Emilia Plain. Ann Geophys 55(4):647–654

Scognamiglio L, Margheriti L, Mele FM, Tinti E, Bono A, De Gori P, Lanciani V, Lucente FP, Mandiello AG, Marcocci C, Mazza S, Pintore S, Quintiliani M (2012) The 2012 Pianura Padana Emiliana seimic sequence: locations, moment tensors and magnitudes. Ann Geophys 55(4):549–555. https://doi.org/10.4401/ag-6159

Servizio Geologico, Sismico e dei Suoli Regione Emilia-Romagna (2012) Terremoto 2012, geologia, rilievi agibilità, analisi dei dati. Edizioni Labanti e Nanni, p 63

Stefani M, Minarelli L (2016) Geological Map of the Province of Ferrara. http://visore.cguferrara.it/Html5Viewer/Index.html?configBase=http://visore.cguferrara.it/Geocortex/Essentials/REST/sites/UNESCO/viewers/VisoreHTML5/virtualdirectory/Resources/Config/Default

Stefani M, Vincenzi S (2005) The interplay of eustasy, climate and human activity in the late Quaternary depositional evolution and sedimentary architecture of the Po Delta system. Mar Geol 222–223:19–48

Tarabusi G, Caputo R (2016) The use of HVSR measurements for investigating buried tectonic structures: the Mirandola anticline, Northern Italy, as a case study. Int J Earth Sci (Geol Rundsch). https://doi.org/10.1007/s00531-016-1322-3

Tertulliani A, Arcoraci L, Berardi M, Bernardini F, Brizuela B, Castellano C, Del Mese S, Ercolani E, Graziani L, Maramai A, Rossi A, Sbarra M, Vecchi M (2012) Emilia 2012 sequence: the macroseismic survey. Ann Geophys 5(4):679–687. https://doi.org/10.4401/ag-6110

Toscani G, Burrato P, Di Bucci D, Seno S, Valensise G (2009) Plio-Quaternary tectonic evolution of the northern Apennines thrust fronts (Bologna-Ferrara section, Italy): seismotectonic implications. Ital J Geosci 128:605–613. https://doi.org/10.3301/IJG.2009.128.2.605